

Self-organization in nonlinear wave turbulence

Richard Jordan^{1,3} and Christophe Josserand^{2,3}

¹ T-7, Los Alamos National Laboratory, Los Alamos, NM 87545

² The James Franck Institute, University of Chicago, 5640 South Ellis, Chicago, Illinois 60637

³ CNLS, Los Alamos National Laboratory, Los Alamos, NM 87545

(March 21, 2022)

We present a statistical equilibrium model of self-organization in a class of focusing, nonintegrable nonlinear Schrödinger (NLS) equations. The theory predicts that the asymptotic-time behavior of the NLS system is characterized by the formation and persistence of a large-scale coherent solitary wave, which minimizes the Hamiltonian given the conserved particle number (L^2 -norm squared), coupled with small-scale random fluctuations, or radiation. The fluctuations account for the difference between the conserved value of the Hamiltonian and the Hamiltonian of the coherent state. The predictions of the statistical theory are tested against the results of direct numerical simulations of NLS, and excellent qualitative and quantitative agreement is demonstrated. In addition, a careful inspection of the numerical simulations reveals interesting features of the transitory dynamics leading up to the long-time statistical equilibrium state starting from a given initial condition. As time increases, the system investigates smaller and smaller scales, and it appears that at a given intermediate time after the coalescence of the soliton structures has ended, the system is nearly in statistical equilibrium over the modes that it has investigated up to that time.

05.20.-y,05.45.-a,52.35.Mw

Submitted to *Physical Review E*

I. INTRODUCTION: NLS AND SOLITON TURBULENCE

A fascinating feature of many turbulent fluid and plasma systems is the emergence and persistence of large-scale organized states, or coherent structures, in the midst of small-scale turbulent fluctuations. A familiar example is the formation of macroscopic quasi-steady vortices in a turbulent large Reynolds number two dimensional fluid [1–3]. Such phenomena also occur for many classical Hamiltonian systems, even though the dynamics of these systems is formally reversible [4]. In the present work, we shall focus our attention on another class of nonlinear partial differential equations whose solutions exhibit the tendency to form persistent coherent structures immersed in a sea of microscopic turbulent fluctuations. This is the class of nonlinear wave systems described by the well-known nonlinear Schrödinger (NLS) equation:

$$i\partial_t\psi + \Delta\psi + f(|\psi|^2)\psi = 0, \quad (1)$$

where $\psi(\mathbf{r}, t)$ is a complex field and Δ is the Laplacian operator. The NLS equation describes the slowly-varying envelope of a wave train in a dispersive conservative system. It models, among other things, gravity waves on deep water [5], Langmuir waves in plasmas [6], pulse propagation along optical fibers [7], and superfluid dynamics [8]. When $f(|\psi|^2) = \pm|\psi|^2$ and eqn. (1) is posed on the whole real line or on a bounded interval with periodic boundary conditions, the equation is completely integrable [9]. Otherwise, it is nonintegrable.

The NLS equation (1) may be cast in the Hamiltonian form $i\partial_t\psi = \delta H/\delta\psi^*$, where ψ^* is the complex conjugate of the field ψ , and H is the Hamiltonian:

$$H(\psi) = \int (|\nabla\psi|^2 - F(|\psi|^2)) \, d\mathbf{r}. \quad (2)$$

Here, the *potential* F is defined via the relation $F(a) = \int_0^a f(y) \, dy$. The dynamics (1) conserves, in addition to the Hamiltonian, the particle number

$$N(\psi) = \int |\psi|^2 \, d\mathbf{r}. \quad (3)$$

We shall assume throughout that eqn. (1) is posed in a bounded one dimensional interval with either periodic or homogeneous Dirichlet boundary conditions. We restrict our attention to attractive, or focusing, nonlinearities

$f(f(a) \geq 0, f'(a) > 0)$ such that the dynamics described by (1) is nonintegrable, free of wave collapse, and admits stable solitary-wave solutions. The dynamics under these conditions has been referred to as *soliton turbulence* [10]. Such is the case for the important power law nonlinearities, $f(|\psi|^2) = |\psi|^s$, with $0 < s < 4$ (in the periodic case, $s \neq 2$ for nonintegrability) [11,12], and also for the physically relevant saturated nonlinearities $f(|\psi|^2) = |\psi|^2/(1 + |\psi|^2)$ and $f(|\psi|^2) = 1 - \exp(-|\psi|^2)$, which arise as corrections to the cubic nonlinearity for large wave amplitudes [13].

Equation (1) in one spatial dimension has solitary wave solutions of the form $\psi(x, t) = \phi(x) \exp(i\lambda^2 t)$, where ϕ satisfies the nonlinear eigenvalue equation:

$$\phi_{xx} + f(|\phi|^2)\phi - \lambda^2\phi = 0. \quad (4)$$

It has been argued [10,14] that the solitary wave solutions play a prominent role in the long-time dynamics of (1), in that they act as *statistical attractors* to which the system relaxes. The numerical simulations in [10], as well as the simulations we shall present within this article, support this conclusion. Indeed, it is seen that for rather generic initial conditions the field ψ evolves, after a sufficiently long time, into a state consisting of a spatially localized coherent structure, which compares quite favorably to a solution of (4), immersed in a sea of turbulent small-scale turbulent fluctuations. At intermediate times the solution typically consists of a collection of these soliton-like structures, but as time evolves, the solitons undergo a succession of collisions in which the smaller soliton decreases in amplitude, while the larger one increases in amplitude. When solitons collide or interact, they shed radiation, or small-scale fluctuations. The interaction of the solitons continues until eventually a single soliton of large amplitude survives amidst the turbulent background radiation. Figure (1) below illustrates the evolution of the solution of (1) for the particular nonlinearity $f(|\psi|^2) = |\psi|$ and with periodic boundary conditions on the spatial interval $[0, 256]$.

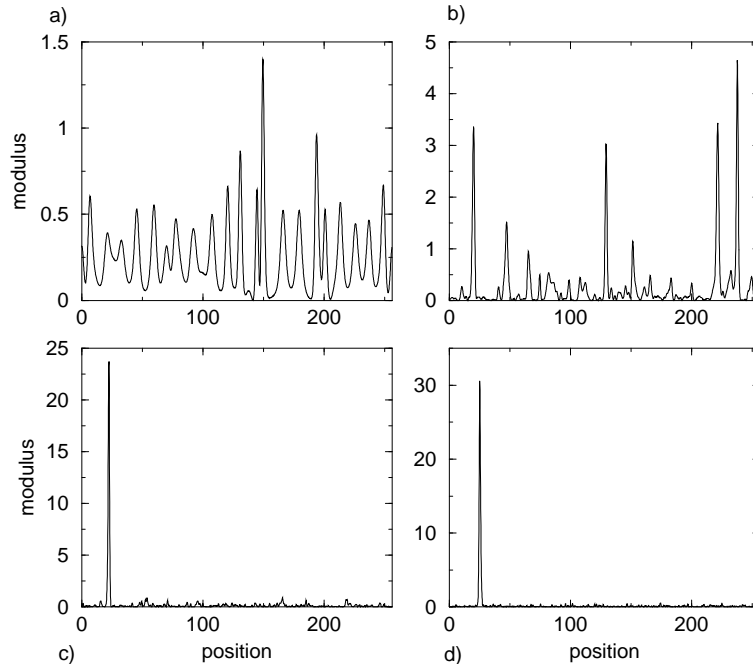


FIG. 1. Profile of the modulus $|\psi|^2$ at four different times for the system (1) with nonlinearity $f(|\psi|^2) = |\psi|$ and periodic boundary conditions on the interval $[0, 256]$. The initial condition is $\psi(x, t = 0) = A$, with $A = 0.5$, plus a small random perturbation. The numerical scheme used to approximate the solution is the split-step Fourier method. The grid size is $dx = 0.125$, and the number of modes is $n = 2048$. a) $t = 50$ unit time: Due to the modulational instability, an array of soliton-like structures separated by the typical distance $l_i = 2\pi/\sqrt{A/2} = 4\pi$ is created; b) $t = 1050$ unit time: The solitons interact and coalesce, giving rise to a smaller number of solitons of larger amplitude; c) $t = 15050$: The coarsening process has ended. One large soliton remains in a background of small-amplitude radiation. Notice that for $t = 55050$ unit time (Figure d)), the amplitude of the fluctuations has diminished while the amplitude of the soliton has increased.

In modeling the long-time behavior of a Hamiltonian system such as NLS, it seems natural to appeal to the methods of equilibrium statistical mechanics. That such an approach may be relevant for understanding the asymptotic-time state for NLS has already been suggested in [10], although the thermodynamic arguments presented by these authors are rather formal and somewhat incomplete. Motivated in part by the ideas outlined in [10], Jordan *et al.* [15] have recently constructed a mean-field statistical theory to characterize the large-scale structure and the statistics of the small-scale fluctuations inherent in the asymptotic-time state of the focusing nonintegrable NLS system (1). The

main prediction of this theory is that the coherent state that emerges in the long-time limit is the ground state solution of equation (4). That is, it is the solitary wave that minimizes the Hamiltonian H given the constraint $N = N^0$, where N^0 is the initial and conserved value of the particle number integral. This prediction is in accord with previous theories [10,14], but the approach taken in [15] is new, and provides a definite interpretation to the notion set forth in the earlier works that it is “thermodynamically advantageous” for the NLS system to approach a coherent solitary wave structure that minimizes the Hamiltonian subject to fixed particle number. The statistical theory also gives predictions for the particle number spectral density and the kinetic energy spectral density, at least for a finite-dimensional spectral truncation of the NLS dynamics (1). In particular, it predicts an equipartition of kinetic energy among the small-scale fluctuations.

In the present work, we shall begin with a brief review of this statistical theory. The predictions of the statistical theory will then be compared in detail with the results of direct numerical simulations of the NLS system. In addition, we will also closely examine the evolution of the particle number spectrum in our numerical simulations, as well as the dynamics (of finite spectral approximations) of the integrals $S_m(\psi) = \int |D^m \psi|^2 dx$ (here D^m denotes the m -th derivative with respect to the spatial variable). The statistical model, being strictly an equilibrium theory, does not give predictions concerning the finite time dynamics of these quantities. However, we shall see that it does give accurate estimates for the long-time saturation values of these quantities for a finite dimensional spectral approximation of the NLS dynamics. In addition, we will demonstrate that the integrals S_m exhibit interesting power law growth in time, as suggested by the weak turbulence theory developed by Pomeau [14].

II. MEAN-FIELD STATISTICAL MODEL

In order to develop a meaningful statistical theory, we begin by introducing a finite-dimensional approximation of the NLS equation (1). To fix ideas and notation, we will consider the NLS system with homogeneous Dirichlet boundary conditions on an interval Ω of length L . Our methods can easily be modified to accommodate other boundary conditions, and we will consider below the predictions of the theory for periodic boundary conditions, as well. In addition, our techniques can easily be extended to higher dimensions, but we wish to concentrate on the one-dimensional case for ease of presentation.

Let $e_j(x) = \sqrt{2/L} \sin(k_j x)$ with $k_j = \pi j/L$, and for any function $g(x)$ on Ω denote by $g_j = \int_{\Omega} g(x) e_j(x) dx$ its j th Fourier coefficient with respect to the orthonormal basis $e_j, j = 1, 2, \dots$. Define the functions $u^{(n)}(x, t) = \sum_{j=1}^n u_j(t) e_j(x)$ and $v^{(n)}(x, t) = \sum_{j=1}^n v_j(t) e_j(x)$, where the real coefficients $u_j, v_j, j = 1, \dots, n$, satisfy the coupled system of ordinary differential equations

$$\begin{aligned} \dot{u}_j - k_j^2 v_j + (f((u^{(n)})^2 + (v^{(n)})^2) v^{(n)})_j &= 0 \\ \dot{v}_j + k_j^2 u_j - (f((u^{(n)})^2 + (v^{(n)})^2) u^{(n)})_j &= 0. \end{aligned} \tag{5}$$

Then the complex function $\psi^{(n)} = u^{(n)} + i v^{(n)}$ satisfies the equation

$$i \psi_t^{(n)} + \psi_{xx}^{(n)} + P^n(f(|\psi^{(n)}|^2) \psi^{(n)}) = 0,$$

where P^n is the projection onto the span of the eigenfunctions e_1, \dots, e_n . This equation is a natural spectral approximation of the NLS equation (1), and it may be shown that its solutions converge as $n \rightarrow \infty$ to solutions of (1) [11,16].

For given n , the system of equations (5) defines a dynamics on the $2n$ -dimensional phase space \mathbf{R}^{2n} . This finite-dimensional dynamical system is a Hamiltonian system, with conjugate variables u_j and v_j , and with Hamiltonian

$$H_n = K_n + \Theta_n, \tag{6}$$

where

$$K_n = \frac{1}{2} \int_{\Omega} ((u_x^{(n)})^2 + (v_x^{(n)})^2) dx = \frac{1}{2} \sum_{j=1}^n k_j^2 (u_j^2 + v_j^2), \tag{7}$$

is the kinetic energy, and

$$\Theta_n = -\frac{1}{2} \int_{\Omega} F((u^{(n)})^2 + (v^{(n)})^2) dx, \tag{8}$$

is the potential energy. The Hamiltonian H_n is, of course, an invariant of the dynamics. The truncated version of the particle number

$$N_n = \frac{1}{2} \int_{\Omega} ((u^{(n)})^2 + (v^{(n)})^2) dx = \frac{1}{2} \sum_{j=1}^n (u_j^2 + v_j^2), \quad (9)$$

is also conserved by the dynamics (5). The factor 1/2 is included in the definition of the particle number for convenience. The Hamiltonian system (5) satisfies the Liouville property, which is to say that the measure $\prod_{j=1}^n du_j dv_j$ is invariant under the dynamics [17]. This property together with the assumption of ergodicity of the dynamics provide the usual starting point for a statistical treatment of a Hamiltonian system [18].

With the finite dimensional Hamiltonian system in hand, we now consider a macroscopic description in terms of a probability density $\rho^{(n)}(u_1, \dots, u_n, v_1, \dots, v_n)$ on the $2n$ -dimensional phase-space \mathbf{R}^{2n} . We seek a probability density that describes the statistical equilibrium state for the truncated dynamics. In accord with standard statistical mechanics and information theoretic principles, we define this state to be the density $\rho^{(n)}$ on $2n$ -dimensional phase space which maximizes the Gibbs-Boltzmann entropy functional

$$S(\rho) = - \int_{\mathbf{R}^{2n}} \rho \log \rho \prod_{j=1}^n du_j dv_j, \quad (10)$$

subject to constraints dictated by the conservation of the Hamiltonian and the particle number under the dynamics (5) [18,19].

The usual canonical ensemble

$$\rho \propto \exp(-\beta H_n - \mu N_n),$$

results from maximizing the entropy subject to the mean constraints $\langle H_n \rangle = H^0$ and $\langle N_n \rangle = N^0$, where H^0 and N^0 are the given values of the Hamiltonian and the particle number, respectively, and β and μ are the Lagrange multipliers to enforce these constraints. However, it has been shown in [15,20] that, for the focusing nonlinearities we consider here, the canonical ensemble is ill-defined in the sense that it is not normalizable (i.e., $\int_{\mathbf{R}^{2n}} \exp[-\beta H_n - \mu N_n] \prod_{j=1}^n du_j dv_j$ diverges). Thus, we are obliged to consider an alternative statistical equilibrium description of the NLS system based on constraints other than those that give rise to the canonical ensemble. The key to constructing an appropriate statistical model is based on the observation from numerical simulations that, for a large number of modes n , in the long-time limit, the field $(u^{(n)}, v^{(n)})$ decomposes into two essentially distinct components: a large-scale coherent structure, and small-scale radiation, or fluctuations. As time progresses, the amplitude of the fluctuations decreases, until eventually the contribution of the fluctuations to the particle number and the potential energy component of the Hamiltonian becomes negligible compared to the contribution from the coherent state, so that N_n and Θ_n are determined almost entirely by the coherent structure. We have checked that this effect becomes even more pronounced when the resolution of the numerical simulations is improved (i.e., when the number of modes is increased with the length L of the spatial interval fixed). On the other hand, as the fluctuations exhibit rapid spatial variations, the amplitude of their gradient does not, in general, become negligible in the asymptotic time limit. Consequently, the fluctuations can make a significant contribution to the kinetic energy component K_n of the Hamiltonian. This is illustrated in Fig. (2).

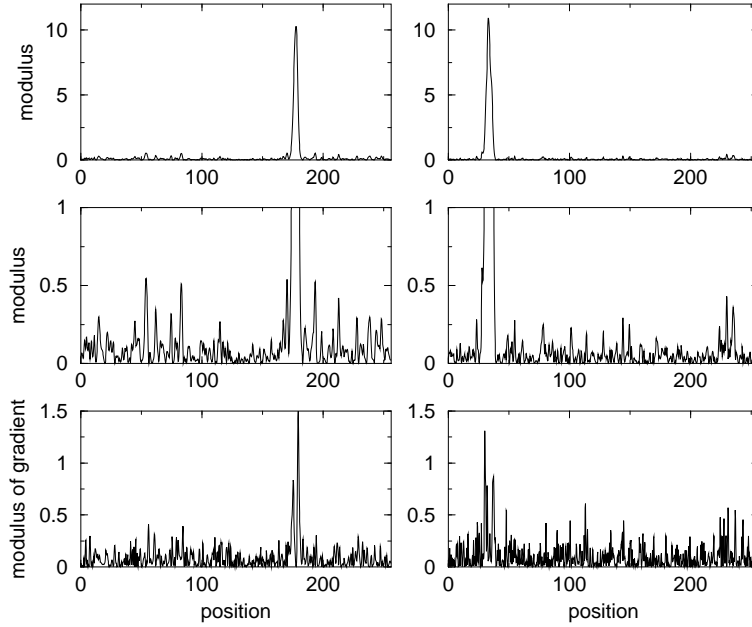


FIG. 2. Numerical simulation for the saturated non-linearity $f(|\psi|^2) = |\psi|^2/(1 + |\psi|^2)$ and for periodic boundary conditions. The total number of modes is $n = 1024$ and the spatial grid size is $dx = 0.25$, so that the length of periodic interval is $L = 256$. Displayed are the modulus of the field $|\psi|^2$ (first and second rows), and the modulus of the gradient of the field $|\psi_x|^2$ (third row) at unit times $t = 30,000$ (left) and $t = 220,000$ (right). The second row shows the same results as the first row, except that the we have restricted the range on the vertical axis in order to focus in on the the fluctuations of the field. Notice that the dynamics for this saturated nonlinearity is qualitatively similar to that for the power law nonlinearity $f(|\psi|^2) = |\psi|$ shown in Fig. (1): the long-time state consists of large-scale coherent solitary wave-like structure interacting with a sea of small-scale fluctuations (top row). The typical amplitude of the fluctuations of the field has decreased from $t = 30,000$ to $t = 220,000$ (second row), while the amplitude of the coherent structure has increased somewhat. The maximum of the modulus of the field is on the order of 50 times larger than the typical modulus of the fluctuations at $t = 220,000$. On the other hand, the typical amplitude of the fluctuations of the gradient of the field has actually increased somewhat from $t = 30,000$ to $t = 220,000$, and the typical amplitude of the fluctuations of the gradient is only several times smaller than the maximum amplitude of the gradient of the field (bottom row). Clearly, the fluctuations make a significant contribution to the kinetic energy in the long-time limit.

Denoting by $\langle u_j \rangle$ and $\langle v_j \rangle$ the means of the variables u_j and v_j with respect to the yet to be determined ensemble $\rho^{(n)}$, we now identify the coherent state with the mean-field pair $(\langle u^{(n)}(x) \rangle, \langle v^{(n)}(x) \rangle) = (\sum_{j=1}^n \langle u_j \rangle e_j(x), \sum_{j=1}^n \langle v_j \rangle e_j(x))$. The fluctuations, or small-scale radiation inherent in the long-time state then correspond to the difference $(\delta u^{(n)}, \delta v^{(n)}) \equiv (u^{(n)} - \langle u^{(n)} \rangle, v^{(n)} - \langle v^{(n)} \rangle)$ between the state vector $(u^{(n)}, v^{(n)})$ and the mean-field vector. The statistics of the fluctuations are encoded in the probability density $\rho^{(n)}$. Based on the considerations of the preceding paragraph, and the results of the numerical simulations displayed in Fig. (2), it seems reasonable to conjecture that the amplitude of the fluctuations of the field $\psi^{(n)}$ in the long-time state of the NLS system (5) should vanish entirely (in some appropriate sense) in the continuum limit $n \rightarrow \infty$. Thus we are led to the following *vanishing of fluctuations hypothesis*:

$$\int_{\Omega} \left[\langle (\delta u^{(n)})^2 \rangle + \langle (\delta v^{(n)})^2 \rangle \right] dx \equiv \sum_{j=1}^n \left[\langle (\delta u_j)^2 \rangle + \langle (\delta v_j)^2 \rangle \right] \rightarrow 0, \text{ as } n \rightarrow \infty. \quad (11)$$

Here, $\delta u_j = u_j - \langle u_j \rangle$ represents the fluctuations of the Fourier coefficient u_j about its mean value $\langle u_j \rangle$, and similarly for δv_j . We emphasize that (11) is a hypothesis used to construct our statistical theory, and not a conclusion drawn from the theory itself.

An immediate consequence of the vanishing of fluctuations hypothesis is that for n sufficiently large, the expectation $\langle N_n \rangle$ of the particle number is determined almost entirely by the mean $(\langle u^{(n)} \rangle, \langle v^{(n)} \rangle)$. Furthermore, the hypothesis (11) implies that for n large, the expectation $\langle \Theta_n(u^{(n)}, v^{(n)}) \rangle$ of the potential energy is well approximated by $\Theta_n(\langle u^{(n)} \rangle, \langle v^{(n)} \rangle)$, which is the potential energy of the mean. This may be seen by expanding the potential F about the mean $(\langle u^{(n)} \rangle, \langle v^{(n)} \rangle)$ in equation (8), taking expectations, and noting that because of the vanishing of fluctuations hypothesis (11), there holds $|\langle \Theta_n(u^{(n)}, v^{(n)}) \rangle - \Theta_n(\langle u^{(n)} \rangle, \langle v^{(n)} \rangle)| = o(1)$ as $n \rightarrow \infty$. Notice, however, that the vanishing of fluctuations hypothesis does not imply that the contribution of the fluctuations to the expectation of the kinetic

energy becomes negligible in the limit $n \rightarrow \infty$. Indeed, this contribution is $(1/2) \sum_{j=1}^n k_j^2 [\langle (\delta u_j)^2 \rangle + \langle (\delta v_j)^2 \rangle]$, which need not tend to 0 as $n \rightarrow \infty$, even if (11) holds. Thus, from these arguments, we conclude that for n sufficiently large, $\langle H_n \rangle \approx \frac{1}{2} \sum_{j=1}^n k_j^2 (\langle u_j^2 \rangle + \langle v_j^2 \rangle) - \frac{1}{2} \int_{\Omega} F(\langle u^{(n)} \rangle^2 + \langle v^{(n)} \rangle^2) dx$. These considerations lead us to impose the following *mean-field constraints* on the admissible probability densities ρ on the $2n$ -dimensional phase space:

$$\begin{aligned} \tilde{N}_n(\rho) &\equiv \frac{1}{2} \sum_{j=1}^n (\langle u_j \rangle^2 + \langle v_j \rangle^2) = N^0 \\ \tilde{H}_n(\rho) &\equiv \frac{1}{2} \sum_{j=1}^n k_j^2 (\langle u_j^2 \rangle + \langle v_j^2 \rangle) - \frac{1}{2} \int_{\Omega} F(\langle u^{(n)} \rangle^2 + \langle v^{(n)} \rangle^2) dx = H^0. \end{aligned} \quad (12)$$

Here, N^0 and H^0 are the conserved values of the particle number and the Hamiltonian, as determined from initial conditions. The statistical equilibrium states are then defined to be probability densities $\rho^{(n)}$ on the phase-space \mathbf{R}^{2n} that maximize the entropy (10) subject to the constraints (12). We shall refer to the constrained maximum entropy principle that determines the statistical equilibria as (MEP).

Further justification and motivation for the vanishing of fluctuations hypothesis (11), which leads to the mean-field constraints in the maximum entropy principle (MEP), are provided in [15]. In particular, it is proved in [15] that the solutions $\rho^{(n)}$ of (MEP) concentrate on the phase-space manifold on which $H_n = H^0$ and $N_n = N^0$ in the continuum limit $n \rightarrow \infty$, in the sense that $\langle N_n \rangle \rightarrow N^0$, $\langle H_n \rangle \rightarrow H^0$, and $\text{var } N_n \rightarrow 0, \text{var } H_n \rightarrow 0$ in this limit. Here, $\text{var } W$ denotes the variance of the random variable W . This concentration property establishes a form of asymptotic equivalence between the mean-field ensembles $\rho^{(n)}$ and the microcanonical ensemble, which is the invariant measure concentrated on the phase-space manifold on which $H_n = H^0$ and $N_n = N^0$. It therefore provides a strong theoretical justification for the mean-field statistical model.

III. CALCULATION AND ANALYSIS OF EQUILIBRIUM STATES

The solutions $\rho^{(n)}$ of (MEP) are calculated by an application of the Lagrange multiplier rule

$$S'(\rho^{(n)}) = \mu \tilde{N}'_n(\rho^{(n)}) + \beta \tilde{H}'_n(\rho^{(n)}),$$

where β and μ are the Lagrange multipliers to enforce that the probability density $\rho^{(n)}$ satisfy the constraints (12). A straightforward but tedious calculation yields the following expression for the maximum entropy distribution $\rho^{(n)}$ [15]:

$$\rho^{(n)}(u_1, \dots, u_n, v_1, \dots, v_n) = \prod_{j=1}^n \rho_j(u_j, v_j), \quad (13)$$

where, for $j = 1, \dots, n$,

$$\rho_j(u_j, v_j) = \frac{\beta k_j^2}{2\pi} \exp \left\{ -\frac{\beta k_j^2}{2} ((u_j - \langle u_j \rangle)^2 + (v_j - \langle v_j \rangle)^2) \right\}, \quad (14)$$

with:

$$\begin{aligned} \langle u_j \rangle &= \frac{1}{k_j^2} (f(\langle u^{(n)} \rangle^2 + \langle v^{(n)} \rangle^2) \langle u^{(n)} \rangle)_j - \frac{\mu}{\beta k_j^2} \langle u_j \rangle \\ \langle v_j \rangle &= \frac{1}{k_j^2} (f(\langle u^{(n)} \rangle^2 + \langle v^{(n)} \rangle^2) \langle v^{(n)} \rangle)_j - \frac{\mu}{\beta k_j^2} \langle v_j \rangle. \end{aligned} \quad (15)$$

Thus, for each j , u_j and v_j are independent Gaussian variables, with means given by the nonlinear equations (15) and with identical variances

$$\text{var } u_j = \text{var } v_j = \frac{1}{\beta k_j^2}. \quad (16)$$

Note that $\text{var } u_j = \langle (\delta u_j)^2 \rangle$ by definition, and likewise for v_j . Obviously, the multiplier β must be positive. Notice also that, since the probability density $\rho^{(n)}$ factors according to (13), the Fourier modes $u_j, v_j, j = 1, \dots, n$, are mutually uncorrelated. In addition, we see from (15) that the complex mean-field $\langle \psi^{(n)} \rangle = \langle u^{(n)} \rangle + i \langle v^{(n)} \rangle$ is solution of (setting $\lambda = \mu/\beta$)

$$\langle \psi^{(n)} \rangle_{xx} + P^n \left(f(|\langle \psi^{(n)} \rangle|^2) \langle \psi^{(n)} \rangle \right) - \lambda \langle \psi^{(n)} \rangle = 0, \quad (17)$$

which is clearly the spectral truncation of the eigenvalue equation (4) for the continuous NLS system (1). It follows, therefore, that the mean-field predicted by our theory corresponds to a solitary wave solution of the NLS equation. Alternatively, the mean $(\langle u^{(n)} \rangle, \langle v^{(n)} \rangle)$ is a solution of the variational equation $\delta H_n + \lambda \delta N_n = 0$, where λ is a Lagrange multiplier to enforce the particle number constraint $N_n = N^0$.

Now, as the maximum entropy distribution $\rho^{(n)}$ is required to satisfy the mean-field Hamiltonian constraint (12), it follows from (13)–(17) that

$$H^0 = \frac{n}{\beta} + H_n(\langle u^{(n)} \rangle, \langle v^{(n)} \rangle). \quad (18)$$

The term n/β represents the contribution to the kinetic energy from the Gaussian fluctuations, and $H_n(\langle u^{(n)} \rangle, \langle v^{(n)} \rangle)$ is the Hamiltonian of the mean. Notice that the contribution of the fluctuations to the kinetic energy is divided evenly among the n Fourier modes. From (18), we obtain the following expression for β in terms of the number of modes n and the Hamiltonian $H_n(\langle u^{(n)} \rangle, \langle v^{(n)} \rangle)$ of the mean:

$$\beta = \frac{n}{H^0 - H_n(\langle u^{(n)} \rangle, \langle v^{(n)} \rangle)}. \quad (19)$$

Using equations (13)–(19), we may easily calculate the entropy of any solution $\rho^{(n)}$ of (MEP). This yields, after some algebraic manipulations, that

$$S(\rho^{(n)}) = C(n) + n \log \left(\frac{L^2 [H^0 - H_n(\langle u^{(n)} \rangle, \langle v^{(n)} \rangle)]}{n} \right). \quad (20)$$

where $C(n) = n - \sum_{j=1}^n \log(j^2 \pi/2)$ depends only on the number of Fourier modes n . Clearly, the entropy $S(\rho^{(n)})$ will be maximum if and only if the mean field pair $(\langle u^{(n)} \rangle, \langle v^{(n)} \rangle)$ corresponding to $\rho^{(n)}$ realizes the minimum possible value of H_n over all fields $(u^{(n)}, v^{(n)})$ that satisfy the constraint $N_n(u^{(n)}, v^{(n)}) = N^0$.

Equation (20) reveals that in statistical equilibrium the entropy is, up to additive and multiplicative constants, the logarithm of the kinetic energy contained in the turbulent fluctuations about the mean state. This result, therefore, provides a precise interpretation to the notions set forth by Zakharov *et al.* [10] and Pomeau [14] that the entropy of the NLS system is directly related to the amount of kinetic energy contained in the small-scale fluctuations, and that it is “thermodynamically advantageous” for the solution of NLS to approach a ground state which minimizes the Hamiltonian for the given number of particles.

We now know that $H_n(\langle u^{(n)} \rangle, \langle v^{(n)} \rangle) = H_n^*$, where H_n^* is the minimum value of H_n allowed by the particle number constraint $N_n = N^0$. As a consequence, the Lagrange multiplier β is uniquely determined by (19):

$$\beta = \frac{n}{H^0 - H_n^*}. \quad (21)$$

That the “inverse temperature” β scales linearly with the number of Fourier modes n is required in order to obtain a meaningful continuum limit $n \rightarrow \infty$ in which the expectations of the Hamiltonian and particle number remain finite. The scaling of the inverse temperature with the number of modes is a common feature of the equilibrium statistical mechanics of finite dimensional approximations of other plasma and fluid systems with infinitely many degrees of freedom, as well [21]. The parameter λ (which depends on n) is also determined by the requirement that the mean $(\langle u^{(n)} \rangle, \langle v^{(n)} \rangle)$ realize the minimum value of the Hamiltonian H_n given the particle number constraint $N_n = N^0$.

Using eqns. (16) and (21), we may now obtain an exact expression for the contribution of the fluctuations to the expectation of the particle number. This is

$$\frac{1}{2} \sum_{j=1}^n [\langle (\delta u_j)^2 \rangle + \langle (\delta v_j)^2 \rangle] = \frac{H^0 - H_n^*}{n} \sum_{j=1}^n \frac{1}{k_j^2} = O\left(\frac{1}{n}\right), \quad \text{as } n \rightarrow \infty. \quad (22)$$

Recall that in the derivation of the mean-field constraints (12), we assumed the vanishing of fluctuations condition (11). The calculation (22) shows, therefore, that the maximum entropy distributions $\rho^{(n)}$ indeed satisfy the hypothesis (11), and hence, that the mean-field statistical theory is consistent with the assumption that was made to derive it. But as the analysis of this section has shown, the maximum entropy distributions $\rho^{(n)}$ provide much more information than is contained in the hypothesis (11). Most importantly, we know that the mean-field corresponding to $\rho^{(n)}$ is an absolute minimizer of the Hamiltonian H_n subject to the particle number constraint $N_n = N^0$. In addition, the

theory yields predictions for the particle number and kinetic energy spectral densities, at least for the $2n$ -dimensional spectrally truncated NLS system (5) with n large. Indeed, we have the following prediction for the particle number spectral density

$$\langle |\psi_j|^2 \rangle = |\langle \psi_j \rangle|^2 + \frac{H^0 - H_n^*}{nk_j^2}, \quad (23)$$

where we have used the identity $\psi_j = u_j + iv_j$, and eqns. (16) and (21). The first term on the right hand side of (23) is the contribution to the particle number spectrum from the mean, and the second term is the contribution from the fluctuations. Since the mean field is a smooth solution of the ground-state equation, its spectrum decays rapidly, so that for $j \gg 1$, we have the approximation $\langle |\psi_j|^2 \rangle \approx (H^0 - H_n^*)/(nk_j^2)$. The kinetic energy spectral density is obtained simply by multiplying eqn. (23) by k_j^2 . As emphasized above, we have the prediction that the kinetic energy arising from the fluctuations is equipartitioned among the n spectral modes, with each mode contributing the amount $(H^0 - H_n^*)/n$.

While we have chosen to present the statistical theory specifically for homogeneous Dirichlet boundary conditions, it is straightforward to develop the theory for NLS on a periodic interval of length L , as well. In this case, it is most convenient to write the spectrally truncated complex field $\psi^{(n)}$ as

$$\psi^{(n)} = \sum_{j=-n/2}^{n/2} \psi_j \exp(ik_j x),$$

for n an even positive integer, where $k_j = 2\pi j/L$. The predictions of the statistical theory remain the same as in the case of Dirichlet boundary conditions. In particular, the mean field $\langle \psi^{(n)} \rangle$ is a minimizer of the Hamiltonian H_n given the particle number constraint $N_n = N^0$, and the particle number spectrum satisfies (23) for $j \neq 0$. The Fourier coefficient ψ_0 may be consistently chosen to be deterministic (i.e., $\text{var } \psi_0 = 0$ and $\langle \psi_0 \rangle \equiv \psi_0$), to eliminate the ambiguity arising from the 0 mode..

IV. NUMERICAL RESULTS

The general predictions of the statistical theory developed above do not depend crucially on the particular nonlinearity f in the NLS equation (1). Indeed, for any f satisfying the conditions stated in the introduction, the coherent structure predicted by the theory in the continuum limit $n \rightarrow \infty$ corresponds to the solitary wave that minimizes the energy for the given number of particles N^0 . Also, for any such nonlinearity f , the particle number spectrum in the long-time limit for the spectrally truncated NLS system (5), according to the statistical theory, should obey the relation (23). Of course, the minimum value H_n^* of the Hamiltonian H_n which enters this formula does depend on f .

Here, we will present numerical results primarily for periodic boundary conditions and for the focusing power law nonlinearity $f(|\psi|^2) = |\psi|$. That is, we shall solve numerically the particular NLS equation

$$i\partial_t \psi + \partial_{xx} \psi + |\psi| \psi = 0, \quad (24)$$

on a periodic interval of length L . We have, however, carried out similar numerical experiments for different focusing nonlinearities and for Dirichlet boundary conditions, and we observed that the general qualitative features of the long-time dynamics are unaltered by such changes. The nonlinearity $f(|\psi|^2) = |\psi|$ actually represents a nice compromise between the focusing effect and nonlinear interactions. For weaker nonlinearities (such as the saturated ones), the interaction between modes is weak, and the time required to approach an asymptotic equilibrium state is quite long. On the other hand, for stronger nonlinearities, the solitary wave structures that emerge exhibit narrow peaks of large amplitude, and therefore, greater spatial resolution is required in the numerical simulations.

The numerical scheme that we use for solving (24) is the well-known split-step Fourier method for a given number n of Fourier modes. Throughout the duration of the simulations, the relative error in the particle number is kept at less than 10^{-6} percent, and the relative error in the Hamiltonian is no greater than 0.1 percent. Notice that the numerical simulations, performed naturally for a finite number of modes, provide an ideal context for comparisons with the mean-field statistical theory outlined above.

On the whole real line, the nonlinear Schrödinger equation (24) has solitary wave solutions of the form $\psi(x, t) = \phi(x)e^{i\lambda^2 t}$, with

$$\phi(x) = \frac{3\lambda^2}{2\cosh^2(\frac{\lambda(x-x_0)}{2})} \quad (25)$$

The particle number N and the Hamiltonian H of these soliton-like solutions are determined by the parameter λ through the relationships $N = 6\lambda^3$ and $H = -\frac{18}{5}\lambda^5$. These solutions are centered at $x = x_0$, as shown in Figure (3), and because of the focusing property of equation (24), as N increases, the amplitude of the solitary wave increases, while its width decreases. For a given value of the particle number N , the solitary wave (25) is the global minimizer of the Hamiltonian H (when the integrals in the definitions (2) and (3) of the Hamiltonian and the particle number extend over the real line). Of course, the solitary wave solutions for the equation (24) on a finite interval, as well as those for the spectrally-truncated version (5), differ from the solution (25) over the infinite interval. However, because the solitary waves (25) exhibit an exponential decay, for a large enough interval, and for a large enough number of modes n , such differences can be neglected for all practical purposes.

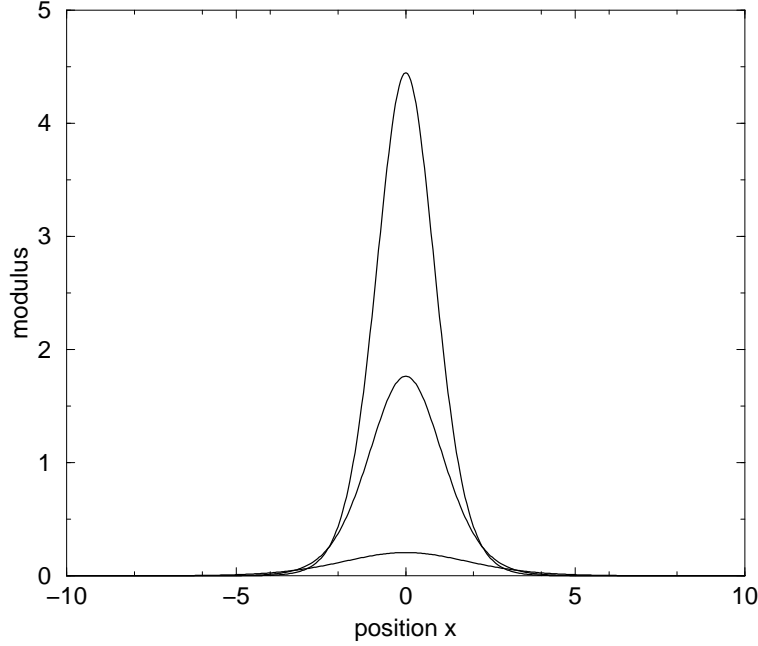


FIG. 3. Solitary wave solutions of equation (24) for particle numbers $N = 1, 5$ and 10 . The modulus $|\psi|^2$ is shown as a function of the position.

For constant A , the condensate $\psi(x, t) = Ae^{iAt}$ is an equilibrium solution of (24). However, since the nonlinearity is focusing, this spatially homogeneous solution is modulationally unstable. Indeed, if we expand ψ around this solution in a series of the form

$$\psi(x, t) = (A + \sum \psi_k e^{(\sigma t + ikx)})e^{iAt}$$

we obtain the dispersion relation:

$$\sigma^2 = Ak^2 - k^4$$

Thus, the condensate is stable for $k^2 > A$, and unstable for $k^2 < A$. The most unstable wave-number is $k_i = \sqrt{A/2}$.

We choose to present in this paper the following set of numerical simulations: starting with the spatially homogeneous solution $\psi(x, t = 0) = A$ (with A of order 1), we add initially a small spatially uncorrelated random perturbation, so that the modulational instability develops. Although we have checked that the long-time behavior of the solution is not dependent on the initial conditions, except through the initial and conserved values N^0 and H^0 of the particle number and the Hamiltonian, this class of initial conditions is particularly convenient for our purposes. For example, by considering different realizations of the initial random perturbation, we may perform an ensemble average over different initial conditions for a given A (and therefore for fixed N^0 and H^0). Such initial conditions provide interesting analogies to standard fluid turbulence problems, as we will emphasize in the conclusion.

The spatially uniform initial conditions we consider here may be thought of as being far away from the expected statistical attractor described by the maximum entropy probability density $\rho^{(n)}$. Indeed, the spectrum of the condensate differs considerably from the predicted statistical equilibrium spectrum (23). The numerical simulations that

we perform here provide strong evidence that the solutions of the spectrally truncated NLS system converge in the long-time limit to a state that may be considered as statistically steady. We shall compare the statistical properties of this long-time state with the predictions of the mean-field statistical theory that was developed and analyzed above. In addition, we shall also investigate the following questions concerning the nature of the evolution leading from the initial state to the long-time statistical equilibrium state: 1- How long does it take for the system to reach the vicinity of its statistical attractor, so that subsequently its statistical features may be considered as stationary? 2- How well can we characterize the “path” that a solution follows en route to the statistically steady state? That is, what are the generic features of the transitory dynamics?

Figure (1) demonstrates that the transitory dynamics can be roughly decomposed into three stages: in the first stage, illustrated in Figure 1 a), the modulational instability creates an array of soliton-like structures separated by a typical distance $l_i = 2\pi/k_i$ associated with most unstable wave number k_i . The second stage is characterized by the interaction and coalescence of these solitons. In this coarsening process, the number of solitons decreases, while the amplitudes of the surviving solitons increase, until eventually a single soliton of large amplitude persists amongst a sea of small-amplitude background radiation (Figures 1 b) and c)). This intermediate stage has previously been observed for other nonlinear Schrödinger equations in one and two spatial dimensions [10,22], and it was shown in [22] that this coarsening process follows a self-similar dynamics. The dynamical exponents of these processes are not very well understood at this point, however. During the final stage of the dynamics, the surviving large-scale soliton interacts with the small-scale fluctuations. As time increases, the amplitude of the soliton increases, while the amplitude of the fluctuations decreases (note the changes from Figure 1 c) to Figure 1 d)). In this stage of the dynamics, the mass (or number of particles) is gradually transferred from the small-scale fluctuations to the large-scale coherent soliton. For a finite number of modes n , the dynamics eventually reaches a “stationary” state whose properties are very well described by the mean-field statistical equilibrium theory developed above, as we shall demonstrate. This implies that long-time state may, in fact, be thought of as a “statistical attractor”, in the sense that, according to the statistical theory, it corresponds to a maximizer of the entropy functional (10) subject to the dynamical constraints (12). Note that because the dynamics is reversible, intermediate states such as those in Figure (1 b) theoretically could still be attained even after the statistical equilibrium state has been reached. In fact, a numerical simulation starting from the state in Fig. (1 d)) but with the time step taken negative shows the reverse dynamics up to round-off errors, where one can observe the decomposition of the solution into an array of soliton-like structures as in figure (1 a)) for intermediate times, while in the limit $t \rightarrow -\infty$ an equilibrium state such as the one of figure (1 d)) is once again attained.

The tendency of the solution of the NLS system (24) to approach the statistical equilibrium state is also captured in the evolution of the kinetic and potential energies (see Figure 4). While the sum of these two quantities, which is the Hamiltonian, remains constant in time, we observe that the kinetic energy increases monotonically, and, consequently, the potential energy decreases monotonically as time goes on. The initial time period where these quantities evolve most rapidly (say $t < 20000$) corresponds to the first two stages of the dynamics described above, in which the modulational instability creates an array of soliton-like structures which then coalesce into a single coherent soliton. After the coalescence has ended, the kinetic (potential) energy increases (decreases) very slowly to its saturation value. In the process, fluctuations develop on finer and finer spatial scales, which accounts for the gradual increase of kinetic energy, while the surviving soliton slowly absorbs mass from the background fluctuations, thereby increasing the magnitude of the contribution to the potential energy from the coherent structure. In the long-time limit, therefore, the soliton accounts for the vast majority of the potential energy, while the fluctuations make a substantial contribution to the kinetic energy.

The mean-field statistical theory provides a prediction for the expected value of the kinetic energy K_n in statistical equilibrium for a given number of modes n . This is $\langle K_n \rangle = K_n(\langle \psi^{(n)} \rangle) + H^0 - H_n^*$, which follows directly upon multiplying eqn. (23) by k_j^2 and summing over j . The first term in this expression for $\langle K_n \rangle$ is the contribution to the mean kinetic energy from the coherent soliton structure which minimizes the Hamiltonian H_n subject to the particle number constraint $N_n = N^0$. The second term in $\langle K_n \rangle$ is the contribution to the expectation of the kinetic energy from the fluctuations. H_n^* is the minimum value of H_n given the particle number constraint. As $n \rightarrow \infty$, we see that $\langle K_n \rangle$ converges to $K(\psi^\infty) + H^0 - H^*$, where ψ^∞ is the minimizer of the Hamiltonian H given the particle number constraint $N = N^0$ for continuous NLS system on the interval $[0, L]$, and $H^* = H(\psi^\infty)$. Approximating $K(\psi^\infty)$ and $H(\psi^\infty)$ by $K(\phi)$ and $H(\phi)$, where ϕ is the solitary wave on the real line whose particle number is N^0 , we obtain for the setting considered in Figure (4) the large n estimates $K_n(\langle \psi^{(n)} \rangle) \approx 9.2$, $H^0 - H_n^* \approx 22.4$, and therefore, $\langle K_n \rangle \approx 31.6$. Also, according to the statistical theory, the expected value $\langle \Theta_n \rangle$ of the potential energy in statistical equilibrium should converge as $n \rightarrow \infty$ to $\Theta(\psi^\infty)$. Approximating this by $\Theta(\phi)$, with ϕ as above, we have the estimate $\langle \Theta_n \rangle \approx -37.1$, which we expect to be accurate for sufficiently large n . We see that the kinetic (potential) energy of the numerical solution is bounded above (below) by the estimate based on the statistical theory, but as expected, the solution does not attain the theoretically predicted value for a finite number of modes. This is because, for the spectrally truncated system, a finite amount of the particle number and the potential energy integrals are actually

contained in the small-scale fluctuations (according to the statistical theory, the contribution of the fluctuations to these quantities should be $O(1/n)$, where n is the number of spectral modes –this follows from (23) [15]). It may be checked that the spatial resolution is improved (i.e., when the number of modes n is increased, while the length L of the spatial interval, and the values H^0 and N^0 of the Hamiltonian and the particle number are held fixed), the contributions of the fluctuations to the particle number and the potential energy decrease, and the saturation values of the kinetic and potential energy attained in the numerical simulations come closer to the predicted statistical equilibrium averages of these quantities (see the inset in Fig. (6), which shows that the saturation value of kinetic energy increases towards the predicted statistical equilibrium value of modes n in the numerical simulation increases). We expect that the contributions of the fluctuations to the particle number and the potential energy should vanish entirely as $n \rightarrow \infty$ for fixed L , H^0 and N^0 , and that the predicted statistical equilibrium values for the mean kinetic energy and potential energy should be approached very closely by the numerical solution in the long-time limit when the number of modes in the simulation is sufficiently large.

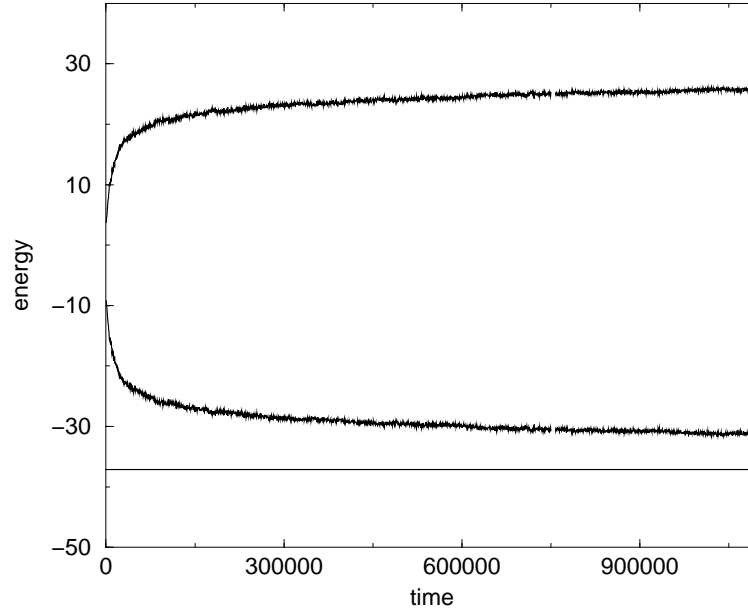


FIG. 4. Time evolution of the kinetic (upper curve) and the potential (middle curve) energies. The kinetic energy is increasing and consequently the potential energy is decreasing, *in accord* with the statistical theory developed above. The lower line indicates the potential energy of the solitary wave that contains all the particles of the system. The curves are obtained from an ensemble average over 16 initial conditions for $n = 512$. The length of the system is $L = 128$, and the (conserved) values of the particle number and the Hamiltonian are, respectively, $N^0 = 20.48$ and $H^0 = -5.46$.

Figures (1) and (4) clearly illustrate that for a given (large) number of modes n , the dynamics converges when $t \rightarrow \infty$ to a state consisting of a large-scale coherent soliton, which accounts for all but a small fraction of the particle number and the potential energy integrals, coupled with small-scale radiation, or fluctuations, which account for the kinetic energy that is not contained in the coherent structure. Formula (23) suggests, in fact, that in the long-time limit, the coherent structure and the background radiation exist in balance (or in statistical equilibrium) with each other, through the equipartition of kinetic energy of the fluctuations. In Figure 5), we display the particle number spectral density $|\psi_k|^2$, where ψ_k is the Fourier transform of the field ψ , as a function of the wave number k for a long time run. To obtain this spectrum, we have performed both an ensemble average over 16 initial conditions, and a time average over the final 1000 time units for each run. For comparison, we have displayed in this figure the spectrum of the solitary wave (25) whose particle number is equal to conserved value of the particle number for the simulation. Observe that there is both a qualitative and quantitative agreement between the spectrum of this solitary wave solution and the small wavenumber portion of the spectrum arising from the numerical simulations. This is in accord with the statistical equilibrium theory, which predicts that the coherent structure should coincide with this solitary wave (in the limit $n \rightarrow \infty$). For larger wavenumbers, the spectrum of the numerical solution is dominated by the small scale fluctuations. We have indicated on the graph the large wavenumber spectrum predicted by the statistical theory. This prediction comes from the second expression on the right hand side of eqn. (23), except that we have approximated the minimum value H_n^* of the Hamiltonian for the spectrally truncated system with n modes by the Hamiltonian H^* of the above-mentioned solitary wave solution for the continuum system. Not only is there

a good qualitative agreement with the predicted equipartition of kinetic energy amongst the small-scale fluctuations (i.e., the k^{-2} slope), but there is also an excellent quantitative agreement between the numerical results and the formula (23) for large k . Let us mention that the long-time spectrum obtained from a single simulation starting from a given initial condition, and without time averaging, though similar to the spectrum displayed in Figure (5), is much noisier.

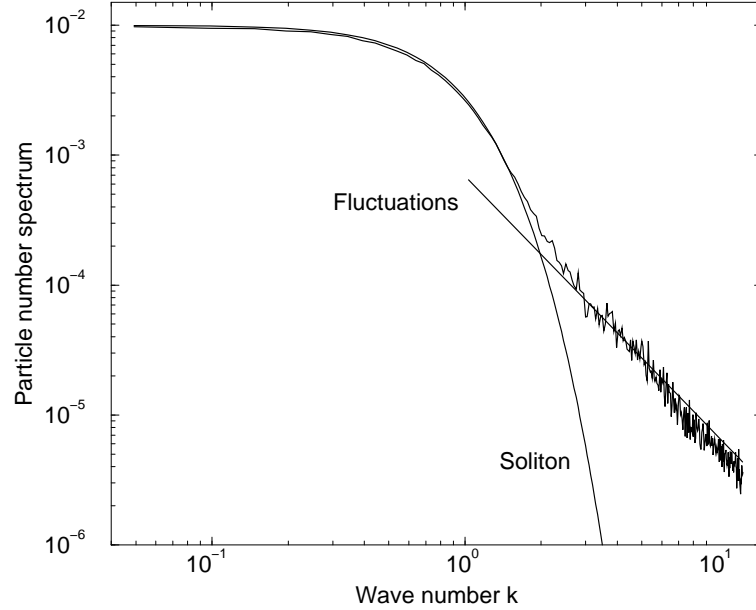


FIG. 5. Particle number spectral density $|\psi_k|^2$ as a function of k for $t = 1.1 \times 10^6$ unit time (upper curve). The lower curve (smooth one) is the particle number spectral density for the solitary wave that contains all the particles of the system. The straight line drawn for large k corresponds to the statistical prediction (23) for the spectral density for large wavenumbers. The numerical simulation has been performed with $n = 512$, $dx = 0.25$, $N^0 = 20.48$ and $H^0 = -5.46$.

As we have mentioned above, the numerical spectrum shown in Figure (5) arises from an ensemble average over long time and over different initial conditions (with the same values of the particle number and the Hamiltonian). Now, under the assumption that the dynamics is ergodic, such an average should coincide with an average with respect to the microcanonical ensemble for the spectrally truncated NLS system [18]. Since it can be shown that the mean-field statistical ensembles $\rho^{(n)}$ constructed above concentrate on the microcanonical ensemble in the continuum limit $n \rightarrow \infty$ (see Theorem 3 of reference [15]), it should be that averages with respect to $\rho^{(n)}$ for large n agree with the ensemble average of the numerical simulations over initial conditions and time, assuming ergodicity of the dynamics. While we have not shown that the dynamics is ergodic, we have, in fact, demonstrated what we believe to be a convincing agreement between the predictions of the mean-field ensembles $\rho^{(n)}$ and the results of direct numerical simulations.

We have also monitored the time evolution of the quantities

$$S_m(\psi^{(n)}) = \sum_j k_j^{2m} |\psi_j|^2, \quad (26)$$

for m a positive integer. For the periodic boundary conditions considered here, the index j ranges from $-n/2$ to $n/2$ and the wavenumber k_j is given by $k_j = 2\pi j/L$. Note that S_1 is the kinetic energy. In general, $S_m(\psi)$ is the squared L_2 norm of the m -th derivative of the field ψ . The growth of S_m in time is an indicator of the development of fluctuations of the field on fine spatial scales. In addition, we may consider that S_m gives an estimate of the evolution of the typical wave number $K(t)$ of the fluctuations since, roughly speaking, we can estimate $S_m \sim K(t)^{2(m-1)}$.

The mean-field statistical theory provides the following prediction for the expectation of S_m in statistical equilibrium for a given number of modes n :

$$\langle S_m \rangle = \sum_{j=-n/2}^{n/2} k_j^{2m} |\langle \psi_j \rangle|^2 + \left(\frac{2\pi}{L} \right)^{2(m-1)} \frac{H^0 - H_n^*}{n} \sum_{j=-n/2}^{n/2} j^{2(m-1)}, \quad (27)$$

where we have used eqn. (23). The first term is the contribution to $\langle S_m \rangle$ from the mean field (the coherent structure), and the second term is the contribution from the fluctuations. Note that for a finite number of modes n , $\langle S_m \rangle$ is finite

for each m , but only $\langle S_1 \rangle$, which is the mean of the kinetic energy, remains finite in the continuum limit $n \rightarrow \infty$. The divergence of $\langle S_m \rangle$ for $m \geq 2$ comes from the second expression on the right hand side of (27) (i.e., from the fluctuations), which is of the order $n^{2(m-1)}$ as $n \rightarrow \infty$. For example, when $m = 2$ this expression is found to be $\pi^2(H^0 - H_n^*)(n^2 + 3n + 2)/(3L^2)$, and we have the following formula for $\langle S_2 \rangle$ for a given number of modes n in the spectrally truncated NLS system:

$$\langle S_2 \rangle = \sum_{j=-n/2}^{n/2} k_j^2 |\langle \psi_j \rangle|^2 + \frac{\pi^2(H^0 - H_n^*)(n^2 + 3n + 2)}{3L^2}. \quad (28)$$

Based on the considerations of the previous paragraph, we expect that the numerical simulations for given number of modes n will reveal that the quantities S_m are bounded and saturate when $t \rightarrow \infty$, but that the larger the number of modes n , the larger the saturation value of S_m (at least for $m \geq 2$). Figure (6) shows the evolution in time of S_2 for different values of n (with the same L , N^0 and H^0). We observe that saturation does indeed occur for a finite number of modes. Also, as n increases, the saturation value increases, as does the time required to reach saturation. By approximating the sum in eqn. (28) by $\int_{-\infty}^{\infty} |\phi_{xx}|^2 dx$ and approximating H_n^* by $H(\phi)$, where ϕ is the solitary wave on the whole real line whose particle number is equal to the conserved particle number for the simulations treated in Figure (6), we obtain the following estimates: $\langle S_2 \rangle \approx 27.1, 45.5, 97.6$ and 170.3 for $n = 48, 64, 96$, and 128 , respectively. Note that these estimates for $\langle S_2 \rangle$ agree closely with the observed saturation values of S_2 in the numerical simulations for $n = 48$ and $n = 64$. For $n = 96$, saturation has not quite yet been reached, but the value of S_2 at the final time $t = 3 \times 10^5$ is still reasonably close to the theoretical estimate of 97.6 . For $n = 128$, S_2 is still growing considerably at the final time of the simulation, and so we can not make comparisons with the statistical prediction for $\langle S_2 \rangle$ at this point. The inset in Figure (6) shows the evolution of the kinetic energy S_1 as a function of time for $n = 48, 64, 96$, and 128 . We see that the kinetic energy saturates nearly at the same rate for all of the values of n considered here. Clearly, S_1 remains bounded as n increases. As discussed above, $\langle S_1 \rangle$, the statistical equilibrium value of the mean kinetic energy, converges as $n \rightarrow \infty$ to $K(\psi^\infty) + H^0 - H(\psi^\infty)$, where ψ^∞ is the solitary wave that minimizes the Hamiltonian H for the given particle number N^0 for the NLS system on the interval $[0, L]$. Once again, approximating ψ^∞ by the solitary wave ϕ on the whole real line that minimizes H given the particle number constraint $N = N^0$, we may estimate the limiting value $\langle S_1 \rangle$ by $K(\phi) + H^0 - H(\phi)$, which is ≈ 7.3 for the value $N^0 = 9.6$ considered in Figure (6). This estimate provides an upper bound on the saturation values of S_1 observed in the simulations, and as the number of modes in the simulations increases, S_1 saturates closer to this approximation of the statistical equilibrium value.

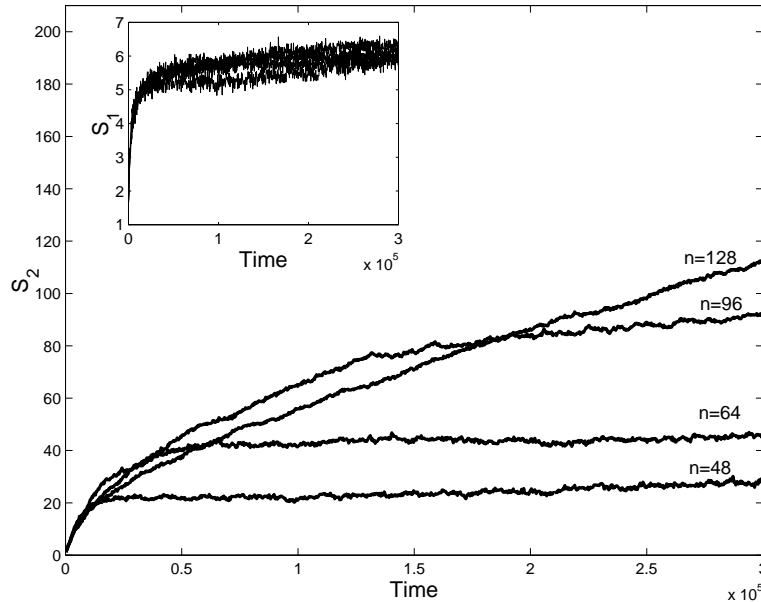


FIG. 6. S_2 as a function of time for $n = 48, 64, 96$ and 128 (lower to upper curve). The simulations are all performed for a box of size $L = 38.4$, for $N^0 = 9.6$ and $H^0 = -3.2$. The curves are obtained from an ensemble average over 16 runs for each n . Saturation is reached for $n = 48$ and $n = 64$, while it is almost obtained for $n = 96$. As n is increased, the time required to reach saturation increases, and the saturation value also increases. The inset shows the kinetic energy S_1 as a function of time for the same values of n . As opposed to S_2 , the saturation of S_1 seems to be occurring at about the same rate for each n . The saturation value of S_1 increases slightly as n increases, but it remains bounded above by the statistical equilibrium value $\langle S_1 \rangle$.

When the spatial resolution of the numerical simulations is improved (i.e, when n is increased with L fixed), the functions S_m are typically seen to exhibit power law growth in time before reaching saturation (see Figure 7).

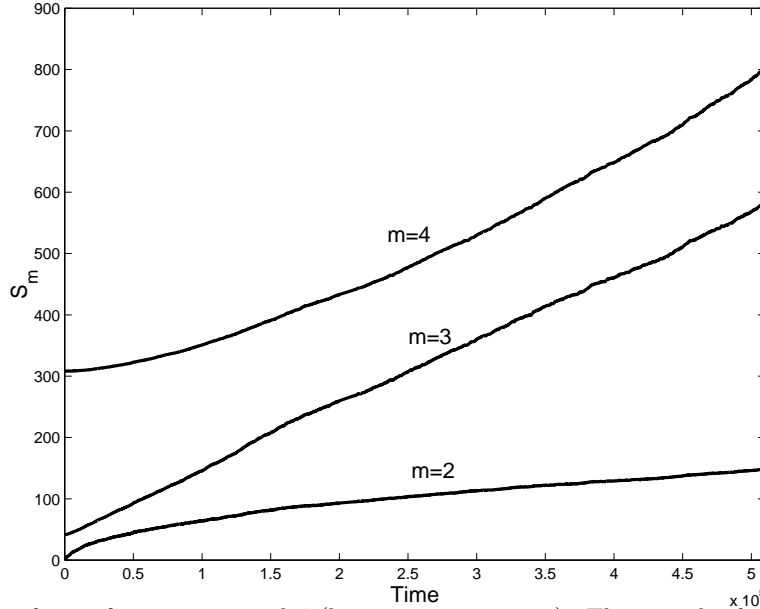


FIG. 7. S_m as a function of time for $m = 2, 3$ and 4 (lower to upper curve). The growth of these quantities is indicative of the development of fluctuations on fine spatial scales as time increases. The S_m have been calculated for 512 modes with $N^0 = 12.8$, $H^0 = -4.26$ and $dx = 0.1$, with an ensemble average over 16 runs. They have been rescaled in order to display them on the same graph.

Indeed, we observe for $m = 2, 3$ and 4 that S_m obeys the following power law dynamics:

$$S_m \propto t^{2(m-1)\nu}, \quad (29)$$

with $\nu = 0.25 \pm 0.01$. This behavior is observed for t large enough that the coalescence process has ended. It corresponds, therefore, to the regime where the kinetic energy has essentially reached saturation. Remarkably, the observed dynamical exponent ν is in good agreement with the prediction of Pomeau [14], which estimates the evolution of the typical wave number $K(t)$ of the fluctuations as time increases. The estimate comes from a dimensional analysis of the weak turbulence equation deduced from equation (24). Describing the fluctuation field $\delta\psi$ as:

$$\delta\psi = \frac{1}{\sqrt{L}} \int dk (\delta I_k)^{1/2} e^{i(kx - \omega t)},$$

the relation between the energy ω and the wave number k is called the spectrum of excitations (we refer the reader to [14] for details). In [14], it has been shown that if this wave number $K(t)$ is in the range where the spectrum of excitations obeys $\omega(k) \sim k^2$, which means that the fluctuations behave essentially like free particles, then, assuming that there is two-wave resonance in the weak turbulence approximation, it follows that $K(t) \sim (\epsilon t)^{1/4}$. Here, ϵ is the spatial energy density of the fluctuations (so $\epsilon \sim (H^0 - H^*)/L$). The analysis in [14] was carried out for cubic defocusing NLS in two spatial dimensions, and does not immediately go over to the case under consideration here. In fact, strictly speaking, in the regime $\omega(k) = k^2$, the resonance of two waves cannot hold in one spatial dimension. However, we conjecture that, due to the interactions with the large-scale coherent structure, the resonance may in fact be meaningful in the present setting, and therefore, we believe that a dimensional weak turbulence analysis along the lines of that developed in [14] may be relevant. We hope to explore this possibility in the future. Interestingly, for the NLS system, the approximation $\omega(k) = k^2$ is usually valid in the limit $k \gg 1$. In the numerical simulations, the finite number of modes provides an ultraviolet cutoff since the largest wave number of the system is

$$k_{max} = \frac{\pi}{dx} = n \frac{\pi}{L}.$$

We remark that we have been able to recognize the power-law growth in time of the quantities S_m only for the smallest dx we have considered in our simulations. For larger dx the free particle regime might not be realized, and it is not surprising in this case that the power law behavior is not observed.

The previous considerations allow us to attach a more precise meaning to what we have been referring to as the transitory dynamics and the equilibrium state for the spectrally truncated NLS system. For sufficiently small grid sizes dx , one may consider that S_m grows according to the power law (29) until the time t_n at which the typical wave number $K(t)$ reaches the largest available wave number k_{max} . This time t_n (which appears to scale as n^4 for fixed L , N^0 and H^0) defines a crossover between the transitory regime in which the solution evolves towards the spectrum (23), and the statistical equilibrium regime where the system investigates its phase-space according to the probability density $\rho^{(n)}$. Notice that in the continuum limit $n \rightarrow \infty$, t_n diverges to infinity, so that continuous NLS system can not reach statistical equilibrium in finite time. Such conjectures are supported by the investigation of the dynamics of the particle number spectrum during the intermediate time regime after which the coarsening process has ended, but before the final statistical equilibrium state has been reached. Note that the statistical equilibrium model does not provide predictions about the time evolution of the spectrum, because it is strictly an equilibrium theory. In fact, based on the statistical theory alone, nothing can be said about path which the system follows from the statistically unlikely initial condition to the final statistical equilibrium state. Figure (8) displays the particle number spectrum at $t = 5 \cdot 10^5$ unit time for a spatial resolution of $dx = 0.1$.

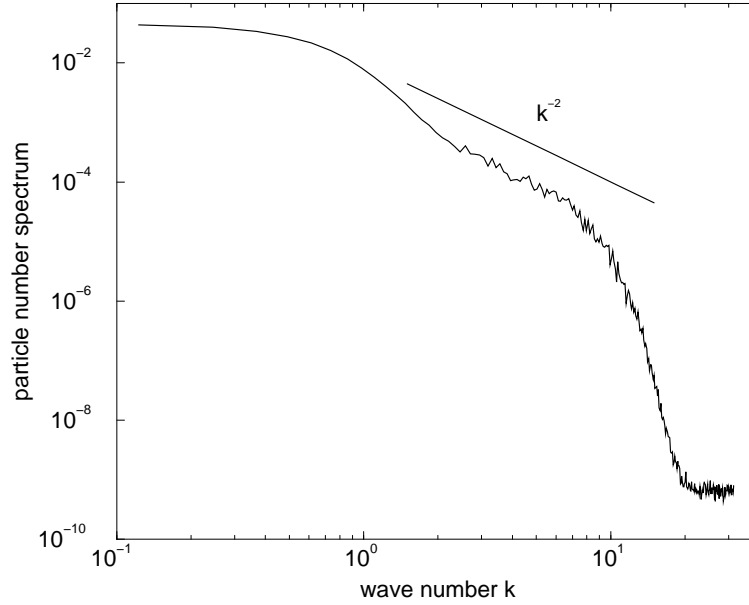


FIG. 8. The particle number spectral density for $n = 512$ and $dx = 0.1$ (thus $L = 51.2$) at unit time $t = 5 \cdot 10^5$. The coherent soliton structure already accounts for almost the entire number of particles of the system, but the system has not yet reached statistical equilibrium. The initial noise level is still present for large wavenumbers ($k \geq 20$), while at smaller wavenumbers, one can recognize both the soliton-like structure and a fluctuation spectrum following approximately a k^{-2} law. The spectrum has been obtained by an ensemble average over 16 initial conditions and a time average over the final 10 unit times.

This figure illustrates that the system investigates smaller and smaller scales as time increases. Indeed, the particle number spectrum for the modes $k \geq 20$ is still at the level of the initial noise. Thus, the smallest scales available to the system have yet to be excited at the time $t = 5 \cdot 10^5$. For larger scales, however, one can recognize both the spectrum corresponding to the coherent soliton structure, and the fluctuation spectrum which appears to follow, at least approximately, the equilibrium law $|\psi_k|^2 \propto k^{-2}$. This suggests the following scenario for the spectrally truncated NLS dynamics: as time increases, smaller and smaller scales are explored, until eventually all available modes are excited. However, at any given time after the coalescence process has ended, the system may be considered as being in statistical equilibrium over all the modes that have been excited up to that point. Defining $k_{max}(t)$ to be the largest wave number that the system has reached up to time t , then we obtain from (29) that $k_{max}(t) \sim (\epsilon t)^{1/4}$, if k_{max} is large enough. Now if we denote by $n(t)$ the number of modes that have been excited up to time t , then based on our previous arguments, we have that $k_{max}(t) = \pi n(t)/L$. But, using $k_{max}(t) \sim (\epsilon t)^{1/4}$, we obtain the following estimate for the spectrum of the fluctuations at time t :

$$\langle |\delta\psi_k|^2 \rangle \sim \frac{H^0 - H^*}{n(t)k^2} \sim \frac{\pi\epsilon^{3/4}}{t^{1/4}k^2}, \quad (30)$$

for $|k| \leq k_{max}(t)$. The total particle number spectrum at time t , of course, has to be taken as the sum of the spectrum

corresponding to the large-scale coherent structure (which decreases exponentially for large k) and the spectrum of the fluctuations.

We emphasize that the derivation of the equation (30) describing the particle number spectrum at an intermediate time t crucially depends on the assumption that the system evolves in such a way that it is nearly in statistical equilibrium over all the modes that have been investigated up to that time. The Figure (8) has motivated us to make this assumption, but clearly further numerical investigations should be carried out in order to test the validity of this hypothesis, as well as the accuracy of the formula (30). Nevertheless, we find it quite interesting that the fluctuation spectrum (30) agrees with the prediction in [14], which was derived from a dimensional analysis of the weak turbulence equations for the NLS system.

V. DISCUSSION-CONCLUSION-ACKNOWLEDGEMENTS.

The primary purpose of the present work has been to test the predictions of a mean-field statistical model of self-organization in a generic class of nonintegrable focusing NLS equations defined by eqn. (1). This statistical theory, which has been summarized above, was originally developed and analyzed in [15]. In fact, we have demonstrated a remarkable agreement between the predictions of the statistical theory and the results of direct numerical simulations of the NLS system. There is a strong qualitative and quantitative agreement between the mean field predicted by the statistical theory and the large-scale coherent structure observed in the long-time numerical simulations. In addition, the statistical model accurately predicts the the long-time spectrum of the numerical solution of the NLS system. The main conclusions we have reached are 1) The coherent structure that emerges in the asymptotic time limit is the solitary wave that minimizes the system Hamiltonian subject to the particle number constraint $N = N^0$, where N^0 is the given (conserved) value of N , and 2) The difference between the conserved Hamiltonian and the Hamiltonian of the coherent state resides in Gaussian fluctuations equipartitioned over wavenumbers.

While the statistical model we have developed is an equilibrium theory, and, strictly speaking, only provides predictions concerning the long-time statistical properties of the NLS system, we have combined this theory with insight gained from numerical simulations to paint a picture of the nature of the dynamics leading up to the statistical equilibrium state. Specifically, the simulations (and, in particular, the results shown in Fig. 8) indicate that evolution is such that, at a given time after the coarsening process has ended, the system is nearly in statistical equilibrium over all the modes that have been excited by that time. From this observation the fact that the quantities S_m defined in (26) are seen to exhibit the power law growth in time according to eqn. (29), we have arrived at the prediction (30) for the time-dependence of the spectrum of the fluctuations. As we have mentioned above, results such as (29) and (30) have previously been derived by Pomeau [14] from weak turbulence arguments, but for the defocusing cubic NLS equation in a bounded two-dimensional spatial domain. We believe that it would be an interesting exercise to check whether these formulas can be derived directly from a weak turbulence analysis in the present context –that is, for 1D nonintegrable focusing NLS equations in the absence of collapse.

We would like to point out certain analogies between the dynamics of the NLS systems we have considered here, and the dynamics of a turbulent 2D Navier-Stokes fluid. A prominent feature of large Reynolds number 2D Navier-Stokes turbulence is the formation of quasisteady coherent vortex structures [1–3]. Starting from generic initial conditions, the evolution of the fluid is characterized by the formation of a collection of large-scale vortices, and the subsequent merger or coalescence of like-signed vortices [3]. The large-scale soliton structures in (focusing, nonintegrable) NLS play a role similar to that of the vortices in 2D Navier-Stokes turbulence. Indeed, we have observed in our numerical simulations of NLS the formation of an array of soliton-like structures which eventually coalesce into a single persistent soliton of large amplitude. Another characteristic feature of turbulence in two-dimensions is the presence of a dual cascade [23]. There is a direct cascade of enstrophy to small scales and an inverse cascade of energy to large scales. As pointed out long ago by Kraichnan [23], the existence of the inverse cascade of energy is indicative of the formation of a large-scale structure in the system. In NLS, there is also a dual cascade. Indeed, our numerical simulations, which correspond to injecting as initial conditions particle number and energy at a given scale l_i associated with the modulational instability, have revealed that there is a direct transfer of kinetic energy to spatial scales smaller than l_i , while the particle number is transferred to large scales. While the 1D NLS equation is much simpler system to investigate, both analytically and numerically, than a turbulent 2D fluid system, we believe that the understanding of the coalescence and transfer processes in this generic model of nonlinear wave turbulence might provide important insight into the nature of turbulent systems in general.

It is a pleasure to thank Robert Almgren, Shiyi Chen, Leo Kadanoff, Yves Pomeau, Bruce Turkington, and Scott Zoldi for valuable discussions and suggestions. R. J. acknowledges support from an NSF Mathematical Sciences Postdoctoral Research Fellowship and from the DOE through a grant to the Center for Nonlinear Studies at Los Alamos National Laboratory. The research of C. J. has been supported by the ASCI Flash Center at the University

- [1] O. Cardoso, D. Marteau and P. Tabeling, *Phys. Rev. E* **49**, 454 (1994); J. Paret and P. Tabeling, *Phys. Fluids* **10**, 3126 (1998).
- [2] M. Rivera, P. Vorobieff and R. Ecke, *Phys. Rev. Lett.* **81**, 1417 (1998).
- [3] J. C. McWilliams, *J. Fluid Mech.* **146**, 21 (1984); D. Montgomery, W. Matthaeus, W. Stribling, D. Martinez, and S. Oughton, *Phys. Fluids A* **4**, 3 (1992).
- [4] A. Hasegawa, *Adv. Phys.* **34**, 1 (1985).
- [5] M. Ablowitz and H. Segur, *J. Fluid Mech.* **92**, 691 (1979).
- [6] H. L. Pesceli, *IEEE Trans. Plasma Sci* **13**, 53 (1985).
- [7] A. Hasegawa and Y. Kodama, *Solitons in optical communications*, Oxford University Press, New York (1995).
- [8] L.P. Pitaevskii, *Sov. Phys. JETP* **13**, 451 (1961); E.P. Gross, *J. Math. Phys.* **4**, 195 (1963).
- [9] V. E. Zakharov and A. B. Shabat, *Soviet Phys. JETP*, 34:62 (1972); Y. Li and D. McLaughlin, *Commun. Math. Phys.* **162**, 175 (1994).
- [10] V. E. Zakharov, A. N. Pushkarev, V. F. Shvets, and V. V. Yan'kov, *JETP Lett.* **48**, 83 (1988); S. Dyachenko, V. E. Zakharov, A. N. Pushkarev, V. F. Shvets, and V. V. Yan'kov, *Soviet Phys. JETP* **69**, 1144 (1989).
- [11] J. Bourgain, *Commun. Math. Phys.* **166**, 1 (1994).
- [12] J. J. Rasmussen and K. Rypdal, *Physica Scripta* **33**, 481 (1986).
- [13] C. E. Max, *Phys. Fluids* **19**, 74 (1976); D. Mihalache, R. G. Nazmitdinov, and V. K. Fedyanin, *Soviet J. Part. Nucl.* **20**, 86 (1989).
- [14] Y. Pomeau, *Nonlinearity* **5**, 707 (1992); Y. Pomeau, *Physica D* **61**, 227 (1992).
- [15] R. Jordan, B. Turkington, and C. Zircel, submitted (1999); <http://xyz.lanl.gov/ps/chao-dyn/9904030>.
- [16] P. E. Zhidkov, *Soviet Math. Dokl.* **43**, 431 (1991).
- [17] B. Bidgary, *Physica D* **82**, 340 (1995).
- [18] R. Balescu, *Equilibrium and Nonequilibrium Statistical Mechanics* Wiley, New York (1975).
- [19] E. T. Jaynes, *Phys. Rev.*, **106**, 620 (1957).
- [20] J. L. Lebowitz, H. A. Rose and E. R. Speer, *J. Stat. Phys.* **50**, 657 (1988).
- [21] J. Miller, P. B. Weichman and M. C. Cross, *Phys. Rev. A* **45**, 2328 (1992); R. Jordan and B. Turkington, *J. Stat. Phys.* **87**, 661 (1997); R. Jordan, Z. Yoshida and N. Ito, *Phys. D* **114** 251 (1998).
- [22] C. Josserand and S. Rica, *Phys. Rev. Lett.* **78**, 1215 (1997).
- [23] R. Kraichnan, *Phys. Fluids* **10**, 1417 (1967).